TORSIONAL-LATERAL MODELING OF COUPLED SYSTEMS BY FINITE ELEMENT TECHNIQUES

Part I - Torsional Analysis

By

E. J. Gunter, Jr.
Professor
Department of Mechanical and Aerospace Engineering
University of Virginia
Charlottesville, VA 22903

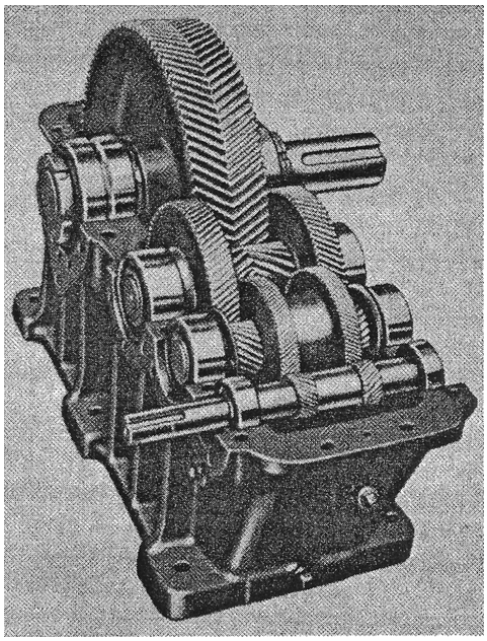

Vibration Institute 20th Annual Meeting
June 24-28, 1996
St. Louis, Missouri

1. BACKGROUND AND INTRODUCTION - TORSIONAL ANALYSIS

The calculation of torsional and lateral vibrations of coupled geared turbomachinery is of considerable interest to the designer due to the high speeds and performance requirements often placed on these units. The calculation of torsional vibrations of rotating and reciprocating machinery represents some of the earliest computations performed on the dynamics of rotors. The torsional vibration problem was an early concern with reciprocating machinery and, later, with the long propeller drive shafts in ships and large coupled systems for utilities and the petrochemical industry.

The analysis of torsional shaft vibrations represents a much simpler problem than does the calculation of the lateral rotor vibrations. For a continuous shaft, the torsional vibrational problem represents a second order differential equation, whereas the lateral vibration problem represents a fourth order partial differential equation for the determination of the natural frequencies and mode shapes. The first successful numerical procedure for the calculation of the torsional vibrations was by the well-known Holtzer method. This method was the earliest of the transfer matrix methods for calculation of vibrations and became very popular since the calculations could be performed by hand for small-degree-of-freedom systems. The transfer matrix method was later extended to the calculation of damped and undamped lateral critical speeds of rotating shafts, as well as forced rotor response.

All transfer matrix methods are a mixed formulation in which both displacements and forces or moments are used in the transformation vector. The simple 2 x 2 Holtzer method, for example, starts with a column vector of slope and torque and propagates across the shaft stations by means of two-by-two transformation matrices. These matrices incorporate the inertia and stiffness elements of the various shaft sections. An initial frequency value is assumed and a characteristic number is computed. This frequency is increased by increments until the characteristic number changes in sign. When this occurs, a natural frequency is determined. The values of the natural frequencies will also depend upon the end boundary conditions of being fixed or free.

Essentially, the Holtzer method is numerically calculating the characteristic polynomial of the system. At every change of sign, a natural shaft frequency is indicated. However, if the step size is too large, then it is possible to skip a natural frequency. Under normal circumstances, this can easily be avoided. Therefore, the Holtzer method for a single-shaft situation is extremely efficient and may be readily programmed on a hand calculator.

The problem in torsional vibrations arises, however, when one has single or multiple branches connected to the main drive shaft. These branches are usually connected through various gears, such as a gearbox or bull gear and pinion system, as in four-poster, double and overhung compressors. For a single-gear reduction system, the Holtzer method is still extremely efficient. The only modification required is that the inertias and shaft stiffnesses are changed by a ratio of speed squared. The main shaft and single-geared system are treated as one single, direct shaft. Where the problem arises in the Holtzer method is with the inclusion of multiple branches. A main shaft must be selected and the other ones are secondary branches. The influence of the local, or constrained, natural frequencies of the branches must be handled very carefully when using the Holtzer method.

In fact, in the use of any transfer matrix method, the branches may cause singular solutions to occur. These singular solutions represent local constrained branch modes which must be accounted for by proper numerical methods. Mathematically, the eigenvalue problem is represented by the characteristic polynomial of the complete system divided by the characteristic polynomials of the various branches. When the iteration frequency is equal to a constrained branch resonance frequency, a singular solution occurs. The local constrained branch frequencies must be first determined and numerically subtracted from the system in order to obtain proper convergence to system modes. Because of the necessity to evaluate the local eigenvalues of multiple branches, the Holtzer method is not attractive for the calculation of the torsional natural frequencies of coupled turborotor systems with complex branches. The effort to make the Holtzer method adapt to this situation is analogous to making the proverbial "silk purse out of a sow's ear."

The finite element method of torsional and torsional-lateral analysis, however, does not suffer from the numerical difficulties encountered with the Holtzer method. The torsional vibration analysis performed by a finite element method represents a direct mass and stiffness formulation. The major drawback to the finite element method previously was the necessity to determine the eigenvalues of nxn matrices, either by such methods as Jacoby, QR for complex damped systems, or by the inverse power method for large systems. This type of analysis has been done very successfully for a number of years by such programs as ***NASTRAN*** on the mainframe computer. With the advancement of the PC computer and certain commercially available finite element codes such as ***MSC/pal2****, ***CDA/sprint****, and ***ANYSYS****, it is now extremely easy and rapid for the designer to calculate the torsional vibrations of extremely complex geared systems. The finite element formulation has the advantage in that the same model may be used for both torsional-lateral and axial vibration analyses. Because the finite

element method essentially generates a complete stiffness and mass matrix for the entire system, the problem of the natural frequencies of the branched components does not arise.

Another advantage of the finite element formulation is that torsional couplings with damping may be readily included in the analysis. A forced synchronous torsional excitation of the system may be performed to determine where the maximum stresses arise and also the relative torsional amplitudes of motion. Depending upon the torsional instrumentation being used, such as strain gauges or laser beams, this provides considerable insight as to the optimum location of where the instrumentation should be placed to monitor the torsional behavior. In general, strain gauges for measuring the torsional stress are not placed at the same location as laser beams to measure the torsional rotation.

There is one type of torsional-lateral vibration effect that will not be dealt with in this paper. In the most general fourth-order differential beam equation, describing coupled lateral, torsional, and axial vibrations, the lateral vibration is coupled to the third derivative by torque and the second derivative of axial loading. The current linear finite element programs do not contain the coupling of the torque through the bending equations. This is a specialty type of situation that may occur in extremely long, slender drill rods used in off-shore drilling platforms. It is not significant in normal rotating machinery. The effect may be observed by placing a rubber hose under a torque, causing the hose to curl into a corkscrew. The type of lateral-torsional coupling that will be presented is through the interaction of gearing, causing simultaneous lateral and torsional excitation.

2. TORSIONAL VIBRATIONS OF A UNIFORM SHAFT

2.1 Continuum Theory

2.1 The problem of torsional vibrations of a uniform shaft is similar in nature to both the problems of shaft axial vibrations and vibrations of a string. Consider Figure 2.1, which represents a uniform shaft element under torsion.

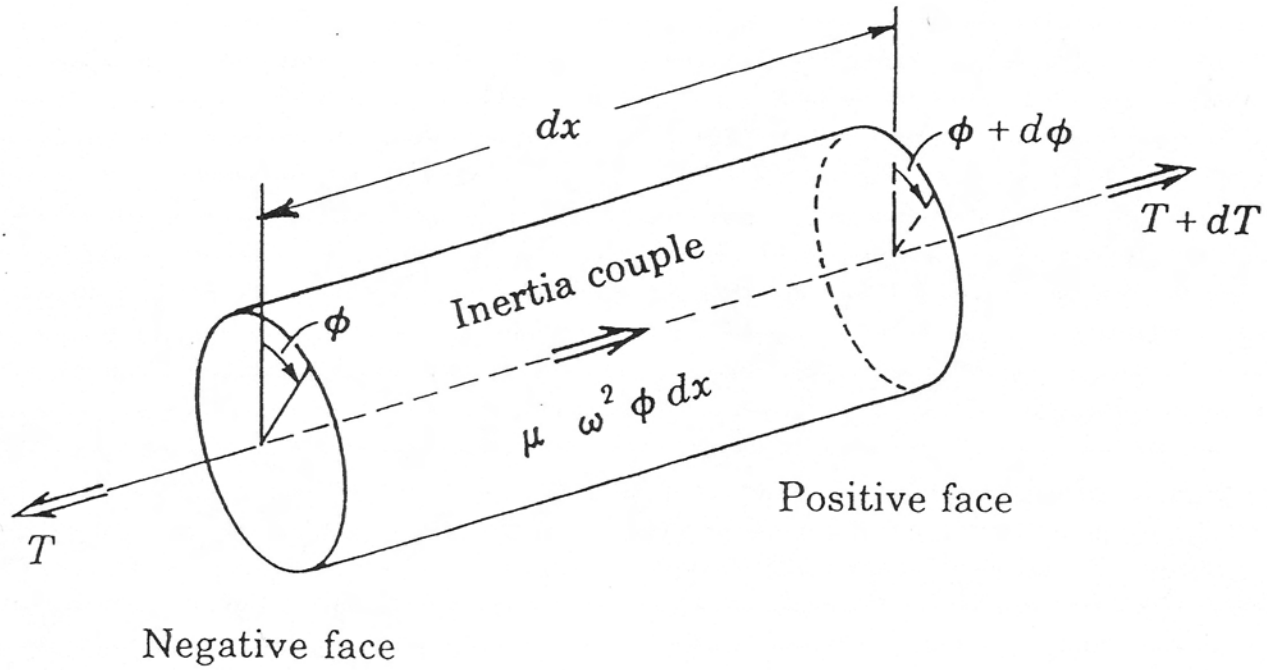

Figure 2.1 Cross-Section of Shaft Element

At the left end of, or negative face of, the cylinder element is acting the torque T_l over the cross-sectional area A. At the right end, the torque T_r is equal to $T + dT$. The torque acting on an incremental element of length dx causes an angular change of $d\phi$ where:

$$\frac{d\phi}{dx} = \frac{T}{JG} \tag{2.1}$$

ϕ =angular twist , rad

T = torque , in-lb

G = shear modulus = $\dfrac{E}{2(1+\nu)}$, Lb-in^2

J = second moment of area, $= \dfrac{\pi D^4}{32}$ for circular shaft, in^4

The shaft angular velocity is $\omega = \dot{\phi}$ and the angular acceleration is $\ddot{\phi}$. The dynamical equation of motion for the shaft element is obtained by summing the external and inertia torques acting on the shaft element as follows:

$$\mu \ddot{\phi}\, dx = dT \tag{2.2}$$

the polar moment of inertia μ per unit shaft length is found by integration:

$$\mu = \int_0^{2\pi}\int_0^{R} \rho r^2 (r\,dr)\, d\phi = \frac{\rho \pi R^4}{2} \tag{2.3}$$

$$= m\frac{R^2}{2}$$

Note:

$m = \rho \pi R^2$, mass/unit length, $M = mL$, total mass

$I_p = \mu L$, total shaft moment of inertia

Thus, substituting back into Equation 2.1

$$\mu \frac{\partial^2 \phi}{\partial t^2} = \frac{dT}{dx} = JG\frac{\partial^2 \phi}{\partial x^2} \tag{2.4}$$

Assuming harmonic motion:

$$\phi(x,t) = \phi(x) e^{i\omega t}$$

The following normalized ordinary second order equation for the angular twist $\{\phi\}$ is obtained for the torsional vibrations of a uniform bar:

$$\frac{d^2\phi}{dX^2} + \lambda^2 \phi = 0$$

Where $\lambda = \dfrac{\mu \omega^2 L^2}{JG}$, $X = \dfrac{x}{L}$

Consider a bar of length L. The general solution to Equation 2.4 may be expressed as:

$$\phi(X) = A \sin\left(\frac{\lambda x}{L}\right) + B \cos\left(\frac{\lambda x}{L}\right) \tag{2.5}$$

with the following boundary conditions:

$$\text{at } x = 0,\ \phi = \phi_{i-1},\ T = T_{i-1}$$
$$\text{at } x = L,\ \phi = \phi_i,\ T = T_i$$
$$\phi(0) = \phi_{i-1} = B$$
$$T(x) = JG\frac{d\phi}{dx} = \frac{JG\lambda}{L}\left[A\cos\left(\frac{\lambda x}{L}\right) - \phi_{i-1}\sin\left(\frac{\lambda x}{L}\right)\right]$$
$$T(0) = T_{i-1} = \frac{JG\lambda}{L}A$$
$$\text{Hence}\quad A = \frac{T_{i-1}L}{JG\lambda}$$

The shaft twist and torque in general are given by:

$$\phi(x) = \phi_{i-1}\cos\left(\frac{\lambda x}{L}\right) + T_{i-1}\frac{L}{\lambda GJ}\sin\left(\frac{\lambda x}{L}\right) \tag{2.6}$$

$$T(x) = T_{i-1}\cos\left(\frac{\lambda x}{L}\right) - \frac{JG\lambda}{L}\phi_{i-1}\sin\left(\frac{\lambda x}{L}\right) \tag{2.7}$$

at x = L, the angular twist ϕ_i and torque T_i are given by:

$$\phi_i = \phi_{i-1}\cos\lambda + T_{i-1}\frac{L}{\lambda GJ}\sin\lambda \tag{2.8}$$

$$T_i = T_{i-1}\cos\lambda - \phi_{i-1}\frac{\lambda GJ}{L}\sin\lambda \tag{2.9}$$

2.2 Natural Frequencies of a Uniform Beam

From Equations 2.8 and 2.9, a transfer matrix formulation based upon continuum mechanics may be formulated for a uniform beam. This process extends easily for the analysis of the natural frequencies of a stepped shaft.

$$\begin{Bmatrix}\phi\\ T\end{Bmatrix}_i = \begin{bmatrix}\cos\lambda & \frac{L}{\lambda JG}\sin\lambda\\ -\frac{\lambda JG}{L}\sin\lambda & \cos\lambda\end{bmatrix}\begin{Bmatrix}\phi\\ T\end{Bmatrix}_{i-1} \tag{2.10}$$

The transfer matrix of Equation 2.10 represents an eigenvalue problem for the determination of the mode shapes and the natural frequencies. For the case of a rotating shaft,

the ends are torque free. The boundary conditions that must be satisfied are that:

$$T_i\,(x = L) = T_{i-1}\,(x = 0) = 0$$

$$T_i = -\frac{\lambda J G}{L} \sin \lambda\, \phi_{i-1} = 0 \tag{2.11}$$

In order for the shaft end at station i to be torque free, it is necessary that:

$$\sin \lambda = 0;\ \lambda = 0,\ \pi,\ 2\pi,\ 3\pi;\ n\pi$$

The values of λ_i are referred to as the eigenvalues of the system. Note that for the case of a continuum, there must exist an infinity of solutions. The normalized mode shapes for the torsional modes for the uniform beam are given by:

$$\phi_n\,(x) = \cos \frac{\lambda x}{L} = \cos \frac{n \pi x}{L}$$

Figure 2.2 represents the first two torsional mode shapes for a uniform shaft. Superimposed on the continuous mode shapes are the modes that result from a lumped three-station model. The requirements for the lumped and finite element models to approach the solution given by continuum mechanics will be discussed in more detail in Sections 2.3 and 2.4.

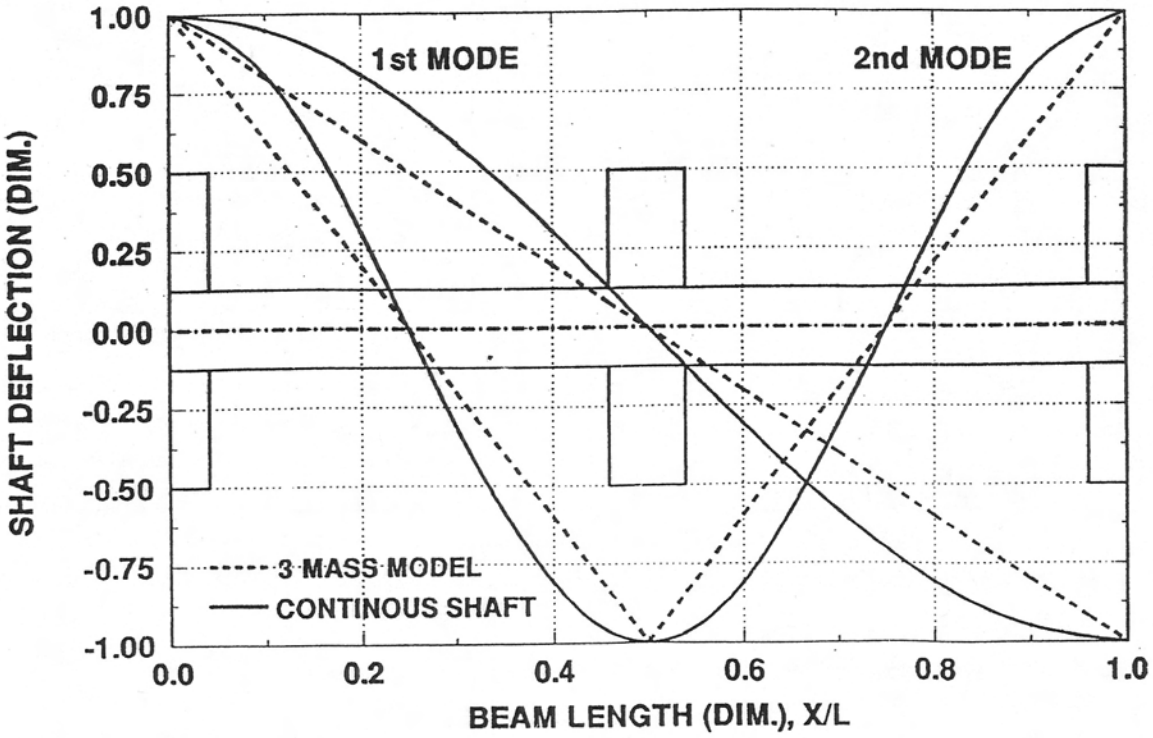

Figure 2.2 1st and 2nd Torsional Mode Shapes for a Continuous Shaft and a 3-Mass Model

Example 2.1

Consider the torsional vibrations of a uniform shaft 60 inches long with a shaft diameter of 6 inches. Assume G = 12E6 lb/in^2 and a shaft mass density of ρ = 7.33E-4 lb-sec^2/in^4 (0.283 / 386 in/sec^2).

$$J = \frac{\pi D^4}{32} = 127.23 \text{ in}$$

$$\frac{GJ}{L} = K_t = \frac{12\text{E}6 \; x \; 127.23}{60} = 2.5447\text{E}7 \text{ in-lb/rad}$$

$$I_p = \mu L = \frac{\rho \pi D^4}{32} L = 5.5931 \text{ lb-in-sec}^2$$

From Equation 2.4 we obtain:

$$\lambda^2 = \frac{\mu \omega^2 L^2}{JG} = (n\pi)^2$$

The torsional natural frequencies ω_n are thus given by:

$$\omega_n = (n\pi)\sqrt{\frac{GJ}{\mu L^2}} \tag{2.12}$$

Thus, for a uniform shaft, the torsional natural frequencies are uniformly spaced as an integer n. This is in contrast to the case of lateral vibrations of a uniform shaft which are spaced n^2.

$$\omega_n = n\pi\sqrt{\frac{K_t}{I_p}} = 6{,}699.8 \; n \text{ rad/sec}$$

N_1 = 1,066.3 CPS
N_2 = 2,132.6 CPS
N_3 = 3,198.9 CPS

Figure 2.2 shows the mode shapes corresponding to the first two torsional modes for a uniform shaft.

2.3 Transfer Matrix Methods

From the equation (2.10), Pestel and Leckie suggest a transfer matrix method for torsional vibrations of stepped uniform shafts.

$$\left\{ Z \right\}_i = \left\{ \begin{matrix} \phi \\ T \end{matrix} \right\}_i = \left[\begin{matrix} \cos \lambda & \frac{L_i}{\lambda J_i G} \sin \lambda \\ -\frac{\lambda J_i G}{L_i} \sin \lambda & \cos \lambda \end{matrix} \right]_{i-1} \left\{ \begin{matrix} \phi \\ T \end{matrix} \right\}_{i-1} \tag{2.13}$$

For the next section, with a change in shaft diameter, we have:

$$\left\{ Z \right\}_{i+1} = \left[T \right]_i \left\{ Z \right\}_i \tag{2.14}$$

For the complete system, we would obtain by substitution:

$$\left\{ Z \right\}_n = \left[T \right]_{n-1} \left[T \right]_{n-2} \cdots \left[T \right]_1 \left[Z \right]_1 \tag{2.15}$$

After the successive 2x2 transfer matrices are multiplied out, we obtain:

$$\left\{ \begin{matrix} \theta \\ T \end{matrix} \right\}_n = \left[\begin{matrix} T_{11} & T_{12} \\ T_{21} & T_{22} \end{matrix} \right] \left\{ \begin{matrix} \theta \\ T \end{matrix} \right\}_1 \tag{2.16}$$

If it is assumed that the ends of the shaft are torque free, then $T_n = T_1 = 0$. In order for this to occur, it is necessary that:

$$T_n = T_{21} (\omega)\, \theta = 0 \tag{2.17}$$

The function T_{2I} is plotted for various values of ω. At each zero crossing of the function, a torsional natural frequency is indicated. Although this procedure works well for a uniform stepped shaft, it does not represent a realistic system, as it does not include the inertia effects of individual wheels or the elasticity of flexible couplings for coupled rotor systems. Also, the transfer matrix, as given by Equation (2.13) for a continuum, represents a potential problem in the term:

$$T_{12\,i} = \frac{L_i}{J_i G} \frac{\sin \lambda}{\lambda}$$

For small values of λ, the ratio of $\frac{\sin \lambda}{\lambda}$ converges to 1. This may not be the case with a computer solution. Numerical round-off may occur.

The product of the point and field matrices yields the complete transfer matrix across the element.

Example 2.2

Consider the uniform beam, as shown in Figure 2.3, divided into two stations.

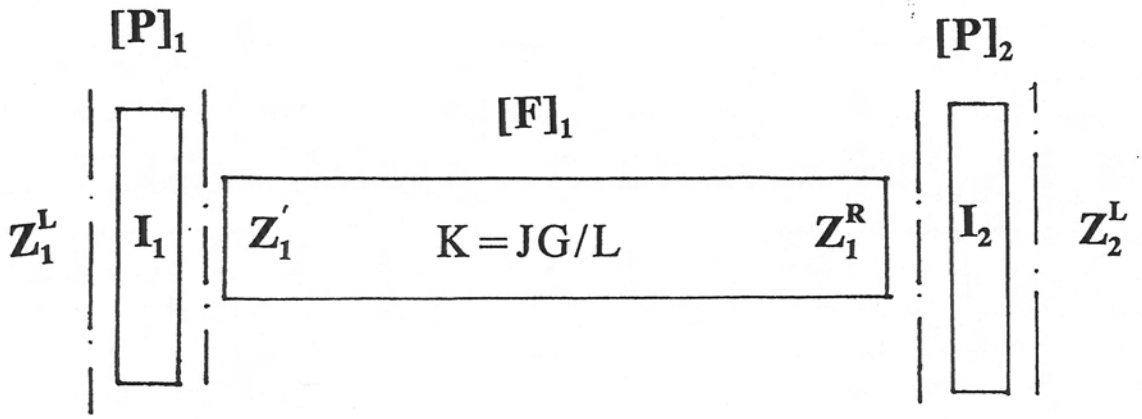

Figure 2.3 Transfer Matrix Stations of a Two-Station System

The transfer matrix across the beam is given by:

$$Z_2^R = \begin{bmatrix} 1 & 0 \\ -\omega^2 I & 1 \end{bmatrix} \begin{bmatrix} 1 & \frac{1}{K} \\ 0 & 1 \end{bmatrix} \begin{bmatrix} 1 & 0 \\ -\omega^2 I & 1 \end{bmatrix} Z_1^L$$

Expanding, we obtain:

$$= \begin{bmatrix} 1 & -\dfrac{\Omega I}{K} & \dfrac{1}{K} \\ -\Omega I \left(2 - \dfrac{\Omega I}{K}\right) & 1 - \dfrac{\Omega I}{K} \end{bmatrix} \begin{Bmatrix} \theta \\ T \end{Bmatrix}_1^L$$

where $\Omega = \omega^2$

To match the boundary conditions that T_2^R must vanish, the system transfer matrix coefficient T_{21} must equal 0.

Therefore,

$$T_{21}(\Omega) = \Omega I \left(2 - \frac{\Omega I}{K}\right) = 0$$

The system natural frequencies are $\Omega_1 = \omega^2 = 0$ and $\Omega_2 = \frac{2K}{I}$

Let $I = n\ I_p$, $K = \frac{GJ}{L}$

Comparing the exact solutions to the approximate, we obtain:

$$\pi^2 \frac{GJ}{LI_p} = \frac{2K}{nI_p}$$

Solving for n:

$$n = \frac{2}{\pi^2} = 0.2$$

Hence, to simulate the influence of the shaft on a torsional critical speed, we would apply 20% of the total shaft I_p for the connecting section at each station. The mode shape connecting each station would be a straight line, as compared to the cosine curve for the exact solution.

The transfer matrix methods, such as the Holtzer method, normally divide the shaft into a series of elements. The moment of inertia of the element is concentrated at a point and the shaft element is considered as massless. This leads to the generation of two matrices called the point and field matrices, respectively, to form the complete element transfer matrix.

$$\{Z\}_n = [P]_n \cdots [F]_2 [P]_2 [F]_1 [P]_1 \{Z\}_1 \qquad (2.18)$$

$$\{Z\}_n = [T]_n \{Z\}_i \qquad (2.19)$$

The transfer matrix $[T]_n$ is a product of the various elements across the entire rotor. For the normal shaft with free-free end conditions, the characteristic determinant of the system is numerically determined by varying ω. For free-free end conditions:

$$\Delta(\omega) = T_{21} = 0 \qquad (2.20)$$

Figure 2.4 represents a typical plot of the Δ function for various values of ω. As shown in Figure 2.4, for each crossing of the axis, causing Δ to equal zero. A natural frequency is obtained. In general, torsional natural frequencies are more evenly spaced then are lateral natural frequencies.

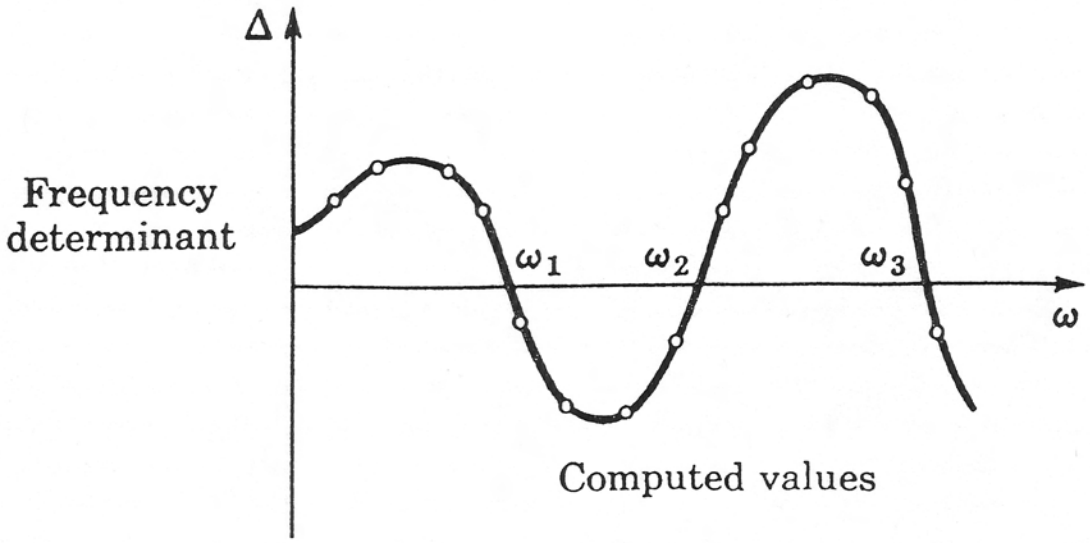

Figure 2.4 Typical Characteristic Determinant as a Function of Frequency

2.4 Direct Matrix Methods

The torsional equations of motion may be represented by a direct matrix formulation. If the polar moment of inertia of the shaft is lumped at stations, and the connecting shaft elements are considered as massless, then the kinetic and potential energy of the system is written as follows:

$$T = \tfrac{1}{2} \sum I_{pi} \dot{\phi}_i^2$$

$$V = \tfrac{1}{2} \sum K_i (\phi_{i+1} - \phi_i)^2 .$$

The equations of motion of the system may be generated by LaGrange's equations, as follows:

$$\frac{d}{dt}\left(\frac{\partial T}{\partial \dot{\phi}_i}\right) - \frac{\partial T}{\partial \phi_i} + \frac{\partial V}{\partial \phi_i} = F_\phi \qquad (2.21)$$

For a 3-mass system, the equations of motion are given by:

$$\begin{bmatrix} I_{p1} & & \\ & I_{p2} & \\ & & I_{p3} \end{bmatrix} \begin{Bmatrix} \ddot{\phi}_1 \\ \ddot{\phi}_2 \\ \ddot{\phi}_3 \end{Bmatrix} + \begin{bmatrix} K_1 & -K_1 & 0 \\ -K_1 & K_1 + K_2 & -K_2 \\ 0 & -K_2 & K_2 \end{bmatrix} \begin{Bmatrix} \phi_1 \\ \phi_2 \\ \phi_3 \end{Bmatrix} = 0$$

EXAMPLE 2.3

Compute the torsional natural frequencies of a 60-inch uniform beam using a 3-mass model:

$$I_{p1} = I_{p3} = \frac{I_p}{4} \; ; \; I_{p2} = \frac{I_p}{2} = 2.798$$

$$K_1 = K_2 = \frac{JG}{L/2} = \frac{1.5268\,\text{E9}}{30} = 5.089\,\text{E7}$$

The natural frequencies are given by:

$$\lambda I_p \begin{bmatrix} \frac{1}{4} & & \\ & \frac{1}{2} & \\ & & \frac{1}{4} \end{bmatrix} \begin{Bmatrix} \phi_1 \\ \phi_2 \\ \phi_3 \end{Bmatrix} = K \begin{bmatrix} 1 & -1 & 0 \\ -1 & 2 & -1 \\ 0 & -1 & 1 \end{bmatrix} \begin{Bmatrix} \phi_1 \\ \phi_2 \\ \phi_3 \end{Bmatrix}$$

where $I_p = 5.594$, $K = 5.089$ E7.

The eigenvalues are:

				% Error
$\lambda_1 =$ 0	$\omega_1 =$ 0 rad/sec	$N_1 =$ 0 CPS		0
$\lambda_2 =$ 3.638 E7	$\omega_2 =$ 6,031.9	$N_2 =$ 960 CPS		-10%
$\lambda_3 =$ 7.276 E7	$\omega_3 =$ 8,530	$N_3 =$ 1,357.6 CPS		-36.3%

With the above lumped mass model, it is seen that the percentage of error in the first mode is -10% and is an excessive -36% for the second mode. It is clear that the 3-mass station model is marginal, even for the representation of the first torsional critical speed.

If the mass, or inertia matrix is formulated based on using a consistent mass matrix, as formulated by finite element theory, then the inertia matrix for the 3-station model is given by:

$$[I] = \frac{I_p}{12} \begin{bmatrix} 2 & 1 & 0 \\ 1 & 4 & 1 \\ 0 & 1 & 2 \end{bmatrix}$$

The resulting eigenvalues, or natural frequencies, are:

		% Error
$N_1 =$	0 CPS	0
$N_2 =$	1,176 CPS	+10.3%
$N_3 =$	2,352 CPS	+10.3%

For a 3-station model, it is seen that the finite element model errors on the high side by 10% for both the 1st and 2nd torsional modes. The consistent mass matrix error is of the same order of magnitude as the lumped mass model, but is substantially more accurate for the second mode (+10%, as compared to -36% error).

For the 3-station uniform beam model, the 1st torsional mode may be computed within 1% accuracy by averaging the lumped mass model and the consistent mass model as follows:

$$[I] = \frac{I_p}{24}\begin{bmatrix} 5 & 1 & 0 \\ 1 & 10 & 1 \\ 0 & 1 & 5 \end{bmatrix}$$

2.5 Finite Element Analysis Of Torsional Natural Frequencies Using PC-Based Finite Element Program

The torsional vibrations of a uniform beam may be rapidly computed on a PC-based finite element program such as ***CDA/sprint®***, ***ANYSYS®***, ***NASTRAN®***, and ***COSMOS®***. The ***CDA/sprint*** program, which has its origins from ***MSC/pal2®***, was chosen to use for the calculations of the torsional vibrations for coupled systems because of its ease of use and understandable command structure. Table 2.1, for example, represents the commands used to generate a model for the calculation of the torsional modes for a 60-inch-long shaft with a diameter of 6 inches. For the model generated by Table 2.1, the shaft has 21 degrees-of-freedom of rotation along the X axis.

The mass and stiffness matrices representing the uniform shaft are square symmetric matrices of order 21 x 21. The stiffness matrix for the torsion problem is a singular matrix. It cannot be inverted because its determinant is zero. This is to be expected, since the first system eigenvalue is 0, which represents the rigid body motion.

There are two methods to determine natural frequencies in ***CDA/sprint***. The first method is by selecting NORMAL MODE analysis, which is a Jacobian method. This method is ideal for systems with singular roots (rigid body modes) and is of small order. For very large order systems, the SUBSPACE ITERATION method should be chosen. Choosing SUBSPACE ITERATION for the file shown in Table 2.1 will result in an error message stating, "***Bad Pivot Element.***" This statement is caused by the singular rigid body rotational mode in the system. There are two techniques to overcome this problem. One may attach a weak torsional spring to the end of the shaft to remove the singularity, or eigenvalues may be shifted away from the singular root by using the SHIFT command in the dynamic analysis.

For a stepped shaft, the command BEAM TYPE 3 D_o, D_i is changed for each change in cross-section. The BEAM TYPE 3 declaration remains in effect until another BEAM TYPE declaration is made.

TABLE 2.1 – *CDA/sprint* COMMANDS FOR TORSIONAL ANALYSIS OF UNIFORM BEAM

```
TITLE        TORSION.TXT
C   CALCULATION OF TORSIONAL NATURAL FREQUENCIES OF A
C   UNIFORM BEAM
C   FREQUENCIES OF A UNIFORM BEAM 60 IN LONG AND 6 IN DIAMETER
NODAL POINT LOCATIONS      1
1     0.0     0.0     0.0     THRU   21     60.0     0.0     0.0     STEP 1
-- BLANK LINE--
C This command generates nodes 1 through 21 evenly spaced along the X axis
C Nodes may also be placed by giving the node #  , xi   ,  yi    ,  zi
C A blank line ends the command.  This is in a global x y z coordinate system

MATERIAL PROPERTIES 30.0E6,  12.0E6,  7.33E4,  0.25
C      MAT                    E      ,     G  ,     ρ  ,     υ
C The MAT command sets the material properties of the system and also dictates
C the system units by the specification of Youngs Modulus E .
C E = 30.0E6 Lb/In^2 , G = 12.0E6 Lb/In^2 ,   ρ = 0.283 Lb/In^3/386 In/Sec^2
C υ = Poissons Ratio = .25

BEAM TYPE 3                6.0     ,     0.0
C Specifies a shaft element with an outside diameter of 6.00 in. and 0 inside diameter
C This element remains in effect until another element is declared
DO CONNECT  1  TO  2  THRU  20  TO  21     STEP  1,  1
C Connects the 1st beam element by nodes 1 & 2 through the 20th beam element
C by nodes 20 & 21 by increments of 1

ZERO 1
TA ALL              !      All translations are eliminated
RY ALL              !      All rotations about the Y axis
RZ ALL              !      All rotations about the Z axis
--BLANK LINE--
C The ZERO command must end in a blank line
C System has initially 6 x 21 degrees of freedom = 126 DOF
C The ZERO command reduces the system to only 21 rotational degrees of freedom
C about the X axis for the analysis of pure torsional vibrations

END DEFINITION
C Last command of the ASCII Build file
```

Figure 2.5 represents the percent error in the calculation of the torsional natural frequencies of a uniform beam by the lumped mass method and by a finite element analysis using consistent mass matrices. With the consistent mass matrix method, the percent error in the calculation of the modes is always on the high side. With the lumped mass method using either a direct stiffness formulation or a transfer matrix method, the error found is always on the negative side, as shown in Figure 2.5.

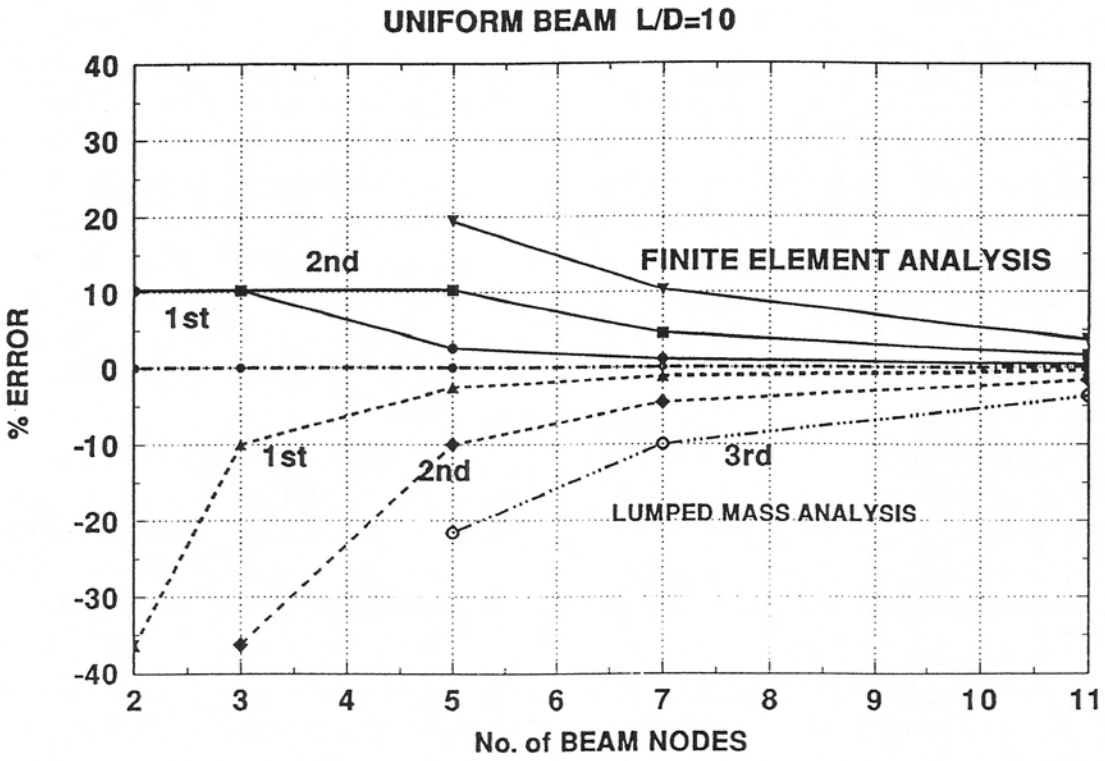

Figure 2.5 Percent Error in Torsional Natural Frequencies for Finite Element and Lumped Mass Methods of a Uniform Beam

For two or three elements, it is seen that the finite element formulation is superior to the lumped mass method. However, when using over five stations, the accuracy of both methods is approximately equivalent with the finite element method, erroring on the high side, and the transfer matrix or lumped mass formulation, erroring on the low side. With four modes, the accuracy of the 1st mode by both methods is less than 1% error and is less than 5% error for the 3rd mode.

Figure 2.6 represents the 1st torsional mode for the uniform 60-inch beam using 20 finite elements. The predicted 1st torsional frequency is at 1067.1 Hz, as compared to the theoretical value of 1066.3 Hz, as shown in Example 2.1. (The 1st torsional mode is actually the system 2nd eigenvalue, as the 1st eigenvalue is a 0 frequency rigid body mode.) For the uniform beam, the first mode has the greatest angular deflection at the ends, but the largest strain at the center. Therefore, laser beam measurements are better suited at the ends, where the largest rotational deflections occur, and strain gauge measurements are best suited at the center.

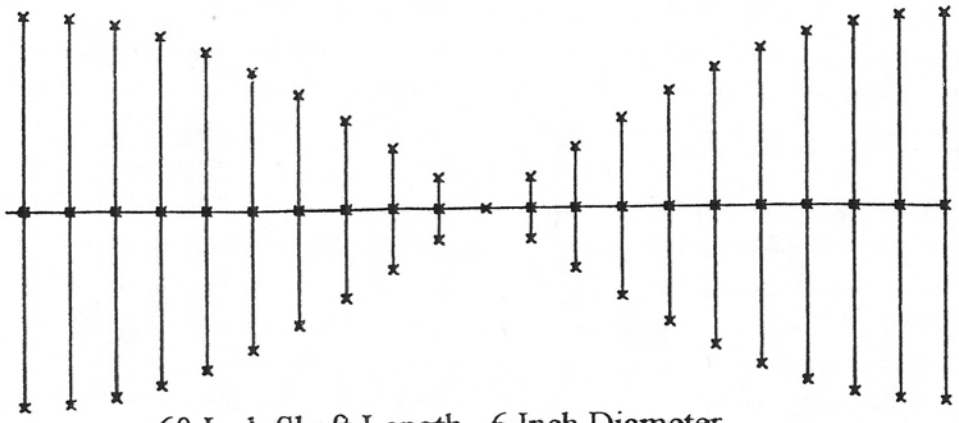

60 Inch Shaft Length , 6 Inch Diameter

Figure 2.6 1st Torsional Mode Shape for a Uniform Beam with 20 Finite Elements - N_1 = 1,067 Hz

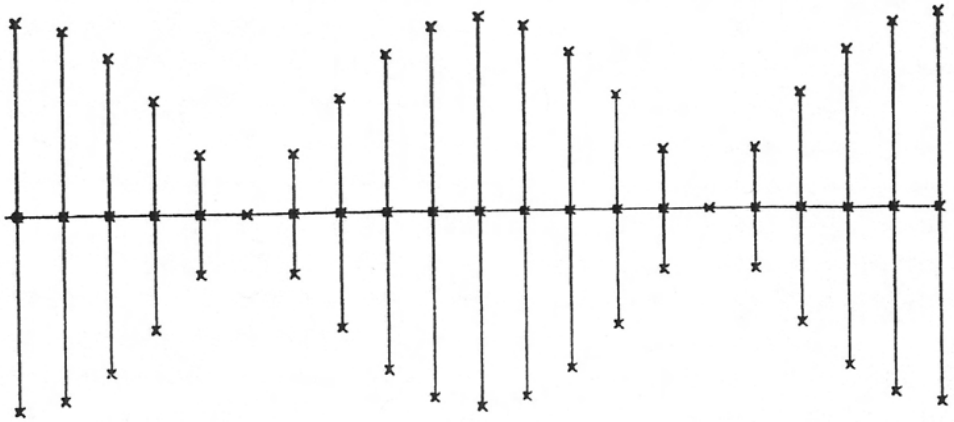

Exact 2 nd Mode = 2,133 Hz

Figure 2.7 2nd Torsional Mode Shape for a Uniform Beam N_2 = 2,141 Hz ; N_2 exact = 2,133 Hz

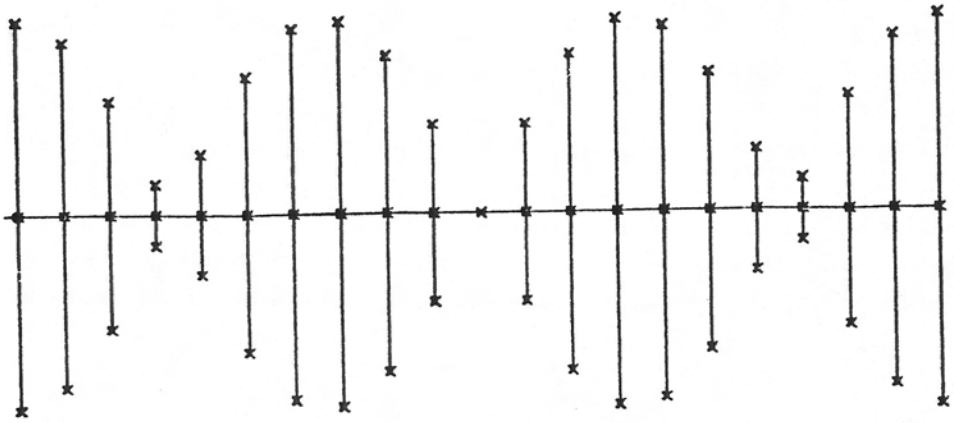

Exact 3 rd Mode = 3,199 Hz

Figure 2.8 3rd Torsional Mode Shape for a Uniform Beam N_3 = 3,228 Hz ; N_3 exact = 3,199 Hz

Figure 2.7 represents the 2nd torsional mode at 2,141 Hz. The exact value for the 2nd torsional is 2,133 Hz. In Figure 2.7, there are two points of zero torsional amplitude at nodes 6 and 16 in the model. Figure 2.8 represents the third mode at 3,228 Hz. In this mode, there are three points of zero amplitude. The 21 stations model requires additional points to obtain the zero amplitude points. The exact solution for this mode is 3,199 Hz, which represents an error of less than 1%.

The torsional vibrations of a shaft may not be as easily visualized as the lateral vibrations. For example, in the finite element programs, one can not directly view torsional motion as one would view a lateral mode shape. The visualization problem can be overcome by the technique of attaching almost massless rods to the shaft and allowing the rods to move freely. The mass of the rods is such that the total inertia is very small in comparison to the shaft. Table 2.2 represents the uniform shaft with light rods attached for animation purposes.

TABLE 2.2 – Torsion Model With Animation Rods

```
TITLE  BEAM21.TXT
C 80 INCH ROTOR WITH 6 INCH DIAMETER - 21 NODES
NODAL POINT LOCATIONS 1                                          ! GENERATE NODE POINTS
1     0.0    0.0    0.0  THRU 21   60.00    0.0    0.0   STEP1 ! 21 NODES FOR 80 IN SHAFT
22    0.0   -10.0   0.0                                         ! NODE FOR BRG #1
23   60.0   -10.0   0.0                                         ! NODE FOR BRG #2
24  -10.0    0.0    0.0                                         ! NODE FOR AXIAL & TORSIONAL
25    0.0   10.0    0.0  THRU 45   60.00   10.0    0.0   STEP1 ! NODES FOR LIGHT BEAMS
46    0.0  -10.0    0.0   THRU 66  60.00  -10.0    0.0   STEP1 ! FOR TORSIONAL ANIMATION
-- BLANK LINE --
MAT 3.0E7,  0,  7.332E-4,  0.3,  3,600,  0,  0                   ! STEEL SHAFT
BEAM TYPE 3,      6.0      0.0                                   ! 6 IN SHAFT
DO CONNECT 1, 2 THROUGH 20, 21     STEP 1, 1                     ! CONNECT UP MAIN SHAFT
MAT 3.0E8,  0.0,     7.33E-6,     0.3                           ! DECLARE LIGHT WEIGHT
                                                                 ! HIGH STIFFNESS
BEAM TYPE 3,        0.1              0.0                         ! THIN BEAM FOR TORSIONAL
                                                                   ANIMATION
DO CONNECT  1,25 THROUGH 21,45   STEP 1,1                        ! CONNECT LIGHT WEIGHT
                                                                   BEAMS FOR ANIMATION
DO CONNECT  1,46 THROUGH 21,66    STEP 1,1
SPRING 1E6                                                       ! RADIAL OR LATERAL SPRING
CONNECT  24 TO 1                                                 ! FOR CRITICAL SPEED ANALYSIS
ZERO 1                                  ! CONSTRAIN SHAFT FOR TORSIONAL MOTION
ALL 24
TY ALL                                  ! DO NOT CONSTRAIN TY FOR LATERAL VIBRATIONS
TX ALL                                  ! DO NOT CONSTRAIN TX FOR LATERAL VIBRATIONS
RY ALL
RZ ALL                                  ! DO NOT CONSTRAIN RZ FOR LATERAL VIBRATIONS
--BLANK LINE--
ZERO 11
TZ 1 THROUGH  21                        ! CONSTRAIN MAIN SHAFT IN Z DIR
-- BLANK LINE--                         ! DO NOT CONSTRAIN LIGHT WEIGHT BARS IN Tz
ACTIVATE 11
RX 1 THROUGH 21                         !* ACTIVATE COMMAND MUST BE USED LAST !
-- BLANK LINE--                         ! ACTIVATE MAIN SHAFT FOR TORSIONAL VIBRATIONS
END DEFINITION                          ! END OF BUILD MODEL
```

3. TORSIONAL VIBRATIONS OF GEARED SYSTEMS

The analysis of the torsional vibrations of a geared system presents difficulties when analyzed by the conventional Holtzer method. In the Holtzer method, one must pick a main branch and the other gear sets are then taken as secondary branches. In the main branch, the system is treated as an equivalent shaft in which the inertia and stiffness components of the attached gear are modified by a speed ratio squared factor. For a single-geared system, this presents no problem. However, if secondary branches are attached, then considerable problems arise with the Holtzer method to make its use unattractive. As shown by Pestel and Leckie (page 162), the branches of a torsional system may cause singular roots. The singular roots correspond to the constrained natural frequencies of the branches.

In the following sections, the natural frequency of a single-geared system will be analyzed and the equivalent system may be constructed by finite element methods using either the ATTACH AT or the OFFSET CONNECT command. These commands allow the construction of a gear set, including teeth flexibility. Once one understands the finite element construction of ATTACH AT to connect two bodies at an offset distance from the construction nodes, then a system with multiple gear sets may be readily constructed.

In the finite element formulation, the problem of the occurrence of singular branch roots is eliminated. In the following sections, the equations of motion for a simple geared system will be presented, with the analytical solution. The analytical solution will be followed by a finite element analysis which will also include the shaft and gear inertias. The key finite element commands which will allow the construction of a geared system are the ATTACH AT and the OFFSET connecting commands. These two commands allow the connection of a spring (gear tooth stiffness) between two nodes (gear centerlines) to be made at the gear interface. By this means, a gear is simulated.

3.1 Equations of Motion of a 2-Gear System

Figure 3.1 represents two shafts connected together through a set of gears. The kinetic energy of the system is given by:

$$T = \tfrac{1}{2}\,\dot{\phi}_1^2\,I_1 + \tfrac{1}{2}\,\dot{\phi}_2^2\,I_2 + \tfrac{1}{2}\,\dot{\phi}_3^2\,I_3 + \tfrac{1}{2}\,\dot{\phi}_4^2\,I_4 \tag{3.1}$$

and the potential energy is given by:

$$V = \tfrac{1}{2}\,K_1\,(\phi_2 - \phi_1)^2 + \tfrac{1}{2}\,K_2\,(\phi_4 - \phi_3)^2 \tag{3.2}$$

If the gears are considered as rigid, then the relationship between the gear motion ϕ_2 and ϕ_3 is given by:

$$R_2\,\phi_2 = R_3\,\phi_3 \text{ and } R_2\,\dot{\phi}_2 = R_3\,\dot{\phi}_3 \tag{3.3}$$

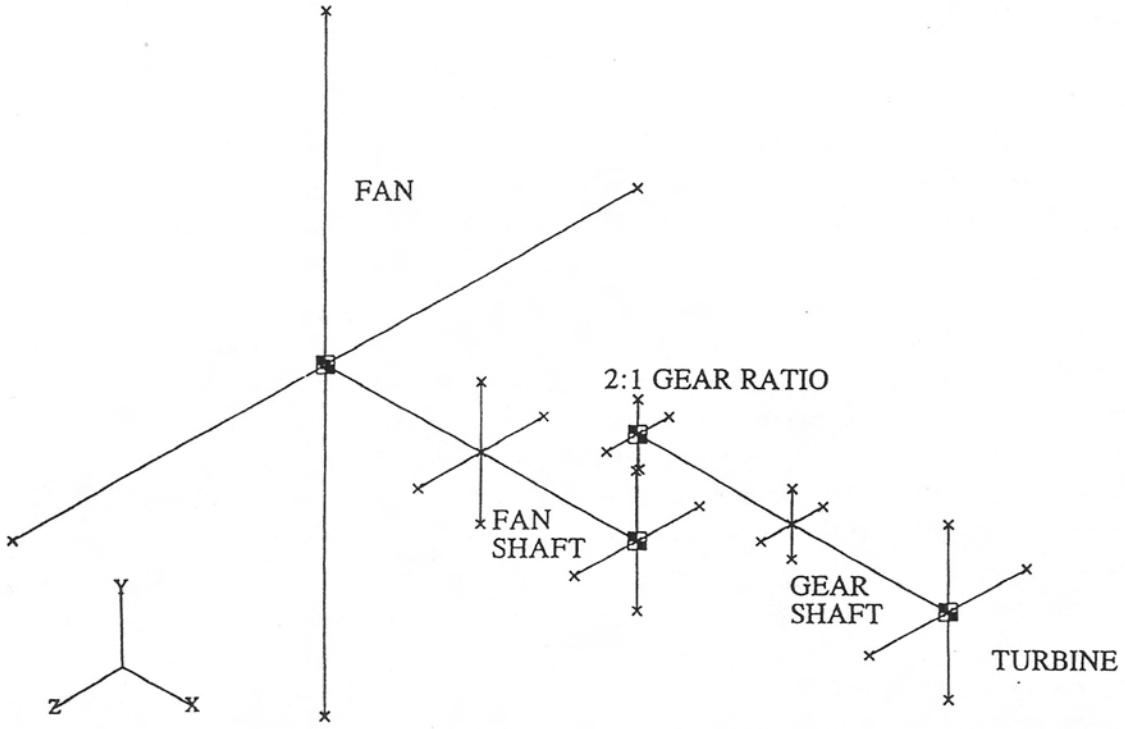

Figure 3.1 2-Shaft Geared Rotor System

Using LaGrange's equation of motion and the above constraint relationship, the system torsional equations of motion are given by:

$$\begin{bmatrix} I_1 & 0 & 0 \\ 0 & I_2 + n I_3 & 0 \\ 0 & 0 & I_4 \end{bmatrix} \begin{Bmatrix} \ddot{\phi}_1 \\ \ddot{\phi}_2 \\ \ddot{\phi}_3 \end{Bmatrix} + \begin{bmatrix} K_1 & -K_1 & 0 \\ -K_1 & K_1 + n K_2 & -n K_2 \\ 0 & -n K_2 & K_2 \end{bmatrix} \begin{Bmatrix} \phi_1 \\ \phi_2 \\ \phi_3 \end{Bmatrix} = 0 \qquad (3.4)$$

where $n = \dfrac{R_2}{R_3}$ = speed ratio

Neglecting gear inertia I_2 and I_3 and assuming $\phi(t) = \phi e^{i\omega t}$, we obtain the characteristic determinant as follows:

$$\begin{bmatrix} K_1 - \omega^2 I_1 & -K_1 & 0 \\ -K_1 & K_1 + n^2 K_2 & -n K_2 \\ 0 & -n K_2 & K_2 - \omega^2 I_4 \end{bmatrix} \begin{Bmatrix} \phi_1 \\ \phi_2 \\ \phi_3 \end{Bmatrix} = 0 \qquad (3.5)$$

3.2 Torsional Natural Frequencies of a 2-Gear System

Expanding at the characteristic polynomial for the system, we obtain:

$$(K_1 - \Omega I_1)\left[(K_1 + n^2 K_2)\ (K_2 - \Omega I_4) - n^2 K_2^2\right]$$

$$- K_1^2 (K_2 - \Omega I_4) = 0 \qquad (3.6)$$

Solving for the roots of Ω:

$$\omega_1 = \sqrt{\Omega_1} = 0 \quad \text{Rigid Body Mode}$$

$$\omega_2 = \sqrt{\Omega_2} = \sqrt{\frac{K_1 K_2 (I_1 + n^2 I_4)}{I_1 I_4 (K_1 + n^2 K_2)}} \quad \text{rad/sec} \qquad (3.7)$$

EXAMPLE 3.1 Torsional Natural Frequency of a 2-Gear System

Wheel 1 D_1 = 10-in diameter, T_1 = 2 in, I_1 = 1.439 lb-in-sec^2
Wheel 2 D_2 = 5-in diameter, T_2 = 1 in, I_2 = 0.045 lb-in-sec^2
L_1 = 10 in, d_1 = 2 in, K_1 = 1.812E6 in-lb
L_2 = 10 in, d_2 = 1 in, K_2 = 0.113E6 in-lb

$$n = 2$$

$$\omega_1^2 = \frac{(I_1 + n^2 I_2)\ (K_1 K_2)}{I_1 I_2\ (K_1 + n^2 K_2)}$$

$$I_1 + n^2 I_2 = 1.619\ ,\ I_1 I_2 = 0.0648$$

$$K_1 + n^2 K_2 = 2.2648\text{E}6\ ,\ K_1 K_2 = 0.2051\text{E}12$$

$$\omega_1^2 = \frac{1.619 \text{ x } 0.2051\text{E}12}{0.0648 \text{ x } 2.2648\text{E}6} = 2.2634\text{E}6$$

$$\omega_1 = 1{,}504 \text{ rad/sec} = 239.56 \text{ Hz}$$

In this example calculation, the inertia of the gears and the connecting shafts are not included. The inclusion of these components is very easy to accomplish. Adding the inertia of the gears and the shaft leads to higher order torsional modes of motion. In Figure 3.1, the two shafts are connected through a set of gears with a speed ratio of R = 2. Figure 3.2 represents the interface of the gear set. In Figure 3.2, the center of gear 1 is at node *a* and the center of gear 2 is at node *b*. If nodes *a* and *b* are simply connected by a spring element, the line of action of the spring face is from node *a* to node *b*.

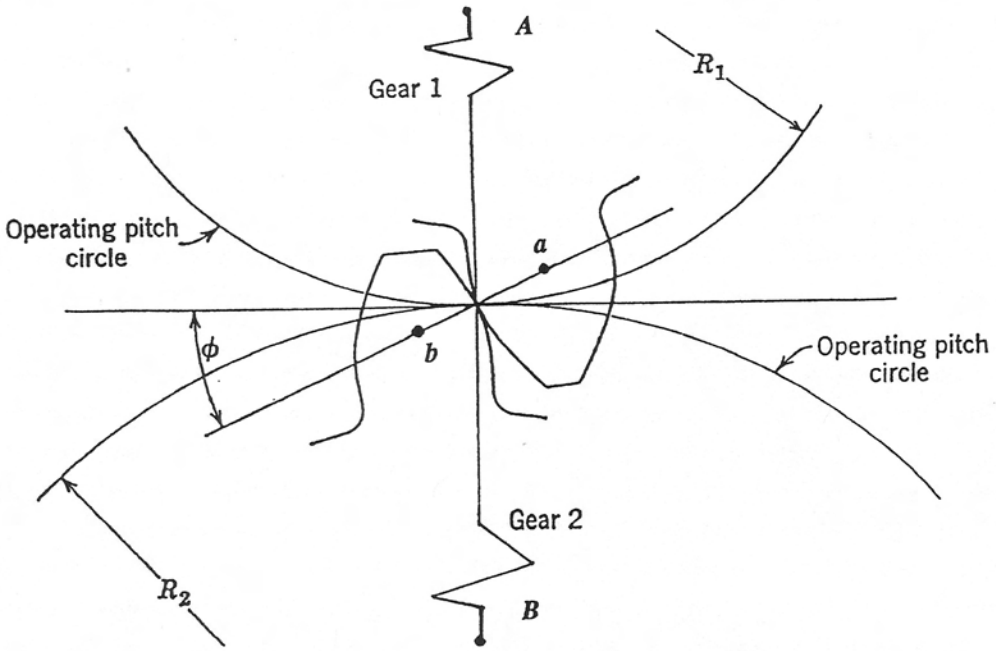

Figure 3.2 Gear Interface Showing Attachment Nodes

In ***CDA/sprint***, there is a command ***ATTACH AT*** which allows the attachment of an element to a rigid body at an offset distance from the geometrical node point. For example, the force action of the two mating gear teeth is along a line of action inclined to the tangent of the operating pitch circle by the angle ϕ. In Figure 3.2, point ***a'*** represents a point on gear 1 along the line of action, and point ***b'*** represents a point on gear 2. A spring is declared to represent the gear tooth stiffness. Table 3.1 represents the basic commands required to attach the disk inertia through the ***MASS*** command and also illustrates the use of the ***ATTACH AT*** command to simulate the action of the gears. A force is generated along the line of action of the points ***a'*** and ***b'*** of gears ***a*** and ***b***. This causes a rotation of the gears about the gear centers and also produces a slight separating force depending upon the assumed angle ϕ of the line of action. In Table 3.1, the two shafts have a diameter of 2.0 inches and 1.0 inch, respectively. After the first shaft is connected, a different size shaft is declared by the ***BEAM TYPE 3*** command. In this file, there are rigid disks attached at stations 1, 3, 6, and 8. The rigid disk is represented by its value of mass M and three mass moment of inertia values I_{uu}, I_{vv}, and I_{ww}. The u, v, and w representations are local coordinates of the element. The v axis is in the direction of the connection of two nodes. Hence, Iuu corresponds to the polar moment of inertia of the disk. The terms I_{vv} and I_{ww} are the transverse moments of inertia of the disk. For a thin disk, we would have that

$$I_{uu} = I_{vv} + I_{ww} = \frac{m R^2}{2}$$

For the analysis of purely torsional vibrations, the transverse moments of inertia I_{vv} and I_{ww} are not required. In Table 3.1, inertia values are included to represent the two gears at nodes 3 and 6. By including the gear inertias and shaft mass, a second torsional is computed at 1,449 Hz. In this mode, the fan and turbine wheels have little motion, but there is considerable motion at the gears. For example, if the turbine had 24 blades and is operating at 60 Hz or 3,600 RPM, then this 2nd mode would be excited by blade passing frequency. This could eventually lead to damage or fretting of the gear teeth.

TABLE 3.1 – Torsional Analysis of 2-Geared System

```
TITLE  TORGEAR2.TXT   TORSIONAL ANALYSIS OF 2 COUPLED SHAFTS
C WHEEL 1 D1=10 IN, T1=2 IN, GEAR 1 = 2 IN RADIUS, GEAR 2 = 1 IN
RADIUS
C WHEEL 2 D2=5 IN, T=1 IN
NODAL POINT LOCATIONS 1
1      0.0,     0.0,     0.0
3      10.0,    0.0,     0.0
6      10.0,    3.0,     0.0
8      20.0     3.0,     0.0
--BLANK LINE--

C MASS NODE   ,   M   ,   Iuu   ,   Ivv   ,   Iww

MASS 1  ,      0.115     ,   1.439          !      Fan MASS and inertia
MASS 3  ,      0.00921   ,  . 01842        !      Gear 1 MASS and inertia
MASS 6  ,      0.00230   ,  0.00115        !      Gear 2 MASS and inertia
MASS 8  ,      0.01439   ,  0.045'         !      Wheel 2 MASS and inertia

MAT 30.0E6  ,   0.0  ,   7.33E-4   ,   0.3

BEAM TYPE 3   2.0
CONNECT 1 TO 2
CONNECT 2 TO 3

BEAM TYPE 3   1.0
CONNECT 6 TO 7
CONNECT 7 TO 8

SPRING 1.0E8

C ATTACH GEAR WITH STIFF SPRING
ATTACH AT 10.0  ,   2.0,   .1 AND 10.0,   2.0   , -.1
CONNECT 3 TO 6

ZERO 1
TA 1,2,3,6,7,8
RY ALL
RZ ALL

END DEFINITION
```

C ATTACH AT COMMAND CONNECTS GEARS AT NODES 3 AND 6 BY MEANS OF OFFSET DISTANCE TO GENERATE MOMENTS ABOUT

3.3 Torsional Analysis of a 3-Spool Rotor System

Figure 3.3 represents a three-level rotor system coupled by a central geared system.

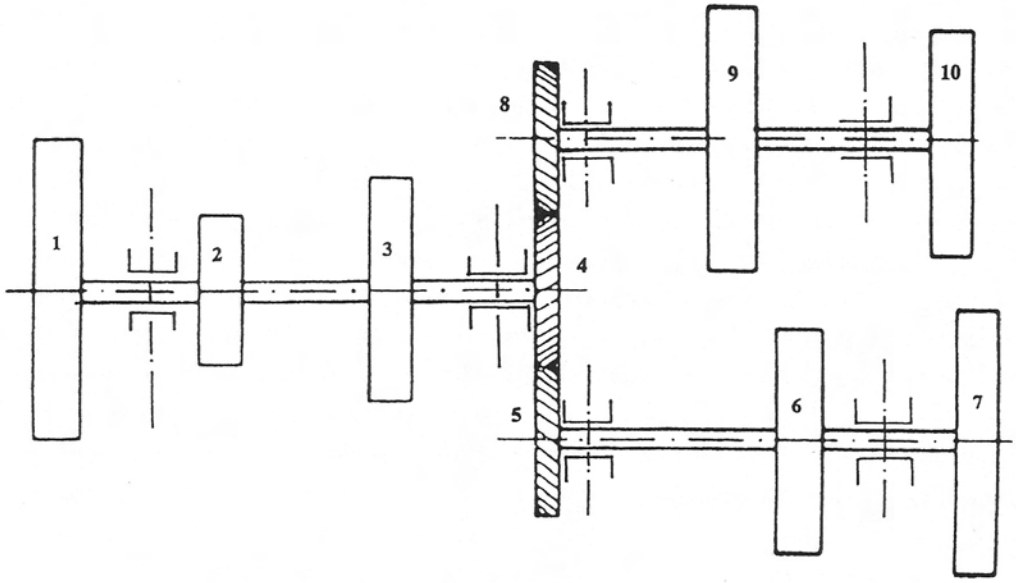

Figure 3.3 Three-Level Coupled Rotor System

If this were analyzed by the Holtzer method, nodes 1 through 7 would be considered as the main branch and nodes 8 through 10 would be taken as a branched system.

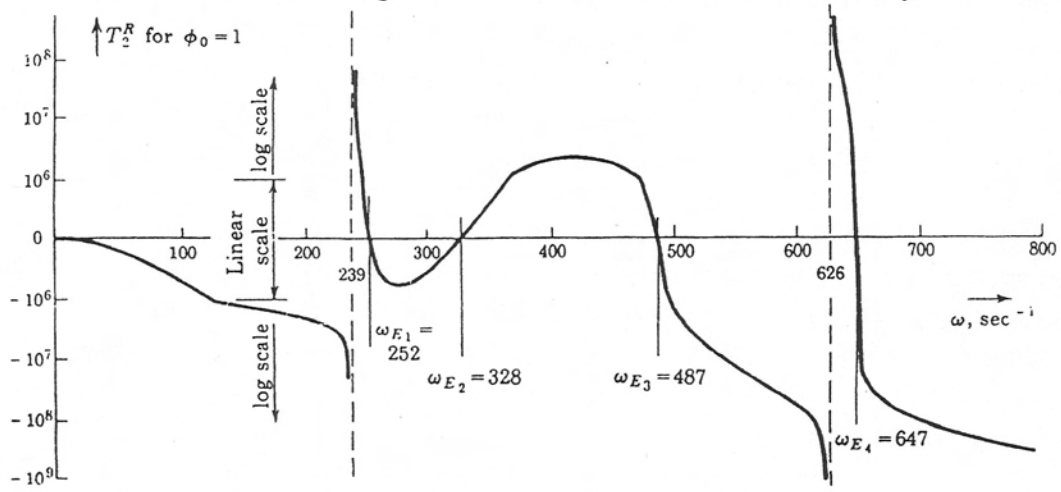

Figure 3.4 Torsional Natural Frequencies and Singular Roots of Coupled Turborotor System Using the Holtzer Method (*Pestel and Leckie*)

Figure 3.4 represents the plot of the characteristic determinant using the Holtzer method. The singular roots at 239 Hz and 626 Hz represent constrained branch modes. These are not true torsional natural frequencies. The natural frequencies are given by the zero crossing points as shown in Figure 3.4.

TABLE 3.2 – Torsional and Torsional-Lateral Modes of a 3-Spool Rotor

Mode No.	Torsional Modes - Hz	Mode No.	Torsional-Lateral Modes - Hz
1	0	1	0
2	28.1	2	17.2
3	37	3	32.1
		4	50.5
		5	54.7
		6	67.6
4	70	7	69.4
		8	72.1
		9	74.6
5	82	10	81.7
		11	86.3
		12	89.1
		13	94.1
		14	110.8
		15	111.8
		16	116.8
		17	117.2
6	122	18	128.9
		19	167.8
		20	176.3

Table 3.2 represents the comparison of the pure torsional modes for the 3-spool rotor and the complete set of modes assuming bearing stiffness of 1E6 lb/in and combined lateral motion, as well as torsional. It is apparent that even in the lower modes, the lateral motion has caused a considerable change in the first two torsional modes. The first torsional mode at 28 Hz drops to 17.2 Hz due to the influence of the bearing flexibility at the gear locations. All the higher modes show strong lateral-torsional coupling.

It is apparent from the observation of Table 3.2, that for a complex geared system, the inclusion of lateral motion with the torsional analysis can cause a considerable deviation in even the pure torsional modes. Many of the lateral modes generate torsional motion from one rotor to another due to the gearing. This implies that radial imbalance could cause torsional excitation, and torsional excitation may link in with the lateral vibration of the connecting rotors at certain modes. These coupling effects of torsional and lateral vibration may be evaluated by finite element methods because of the ability to offset connect elements to represent gears. This type of coupling is impossible to easily represent by a Holtzer or transfer matrix method. For the analysis of torsional-lateral vibrations of complex geared systems, it is apparent that a finite element method is the preferred method of analysis.

Figure 3.5 represents the 1st system torsional critical speed at 17.2 Hz. In this model, bearing stiffnesses of 1E6 lb/in were assumed for all bearings. The interaction of the gear reactions with the bearings causes lateral shaft deflections at the bearings located near the gears. This leads to a considerable reduction in both the 1st and 2nd torsional critical speeds (system 2nd and 3rd modes).

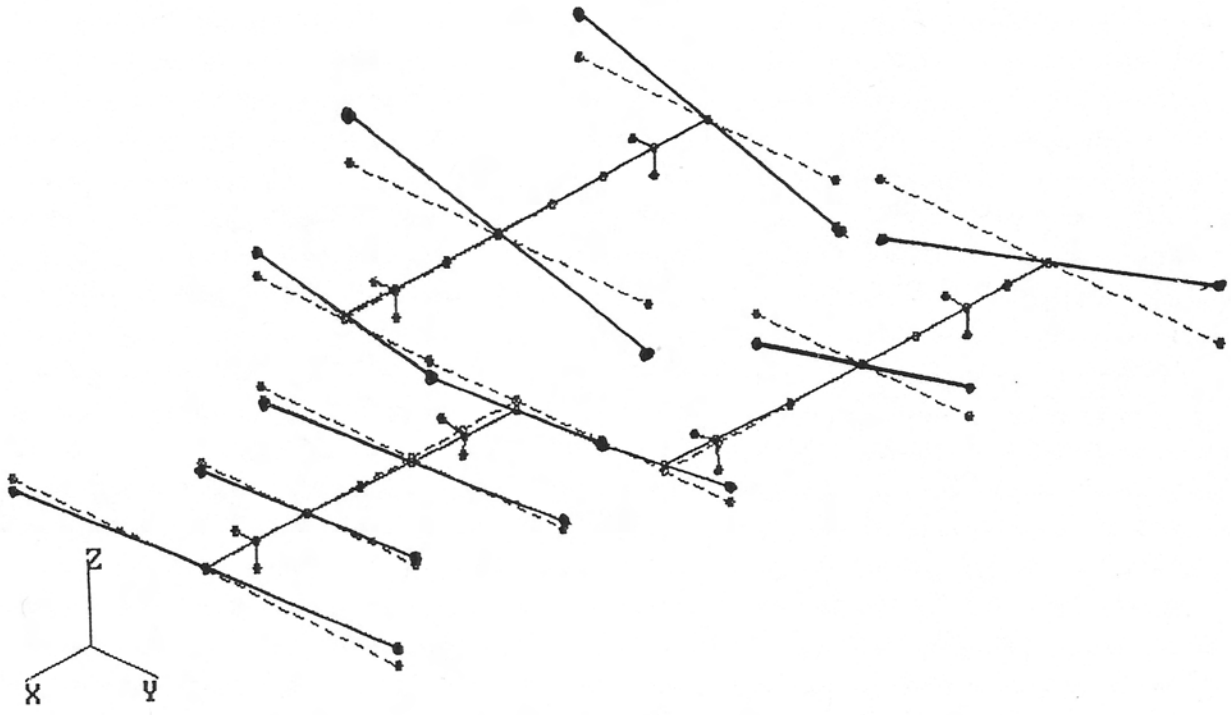

Figure 3.5 3-Shaft System 1st Torsional Critical Speed at 17.2 Hz With Lateral Motion Included

4. SUMMARY AND CONCLUSIONS

In this paper, a procedure was presented for the calculation of the torsional critical speeds of gear coupled rotor systems by finite element techniques. The Holtzer method, which has been traditionally used for the calculation of torsional speeds, is greatly flawed for use in calculation of the torsional criticals in geared systems. This is because of the singularities which arise due to the local resonances that occur in the branches for the Holtzer method. The finite element methods, such as the ***CDA/sprint*** program, allow the generation of geared sets by means of the ***ATTACH AT*** or ***OFFSET CONNECT*** commands. All the roots of the system may be found with equal accuracy. The torsional situation becomes more complex when lateral motion is included with the torsional. The paper presents a three-level rotor showing the difference in the torsional critical speeds with lateral motion included. There can be a considerable reduction in the torsional critical speeds and the higher modes show considerable interaction between the lateral and torsional motion. Although this paper has only dealt with the undamped torsional motion, the finite element process allows the calculation of forced response, including torsional damping at couplings. The forced response of torsional-lateral systems, including torsional damping, will be discussed in a future paper.

REFERENCES

1. Bathe, K. and E. L. Wilson. ***Numerical Methods in Finite Element Analysis***, Prentice Hall, NJ, 1976.
2. Chen, W. J. ***DYROBES – Dynamics of Rotor Bearing Systems User's Manual***, Ver. 4.21, Rodyn Vibration Analysis, Inc., 1932 Arlington Boulevard, Charlottesville, VA, 1995.
3. Cohen, R. B. and E. J. Gunter. ***Undamped Torsional Critical Speed Analysis of Rotor Systems – A Manual for Use with Computer Program CRITSPD***, Report No. UVA/643078/MAE 811105, June 1981.
4. Den Hartog, J. P. ***Mechanical Vibrations***, McGraw Hill, New York, 1947.
5. Ehrich, F. F. Editor, ***Handbook of Rotordynamics***, McGraw Hill, New York, 1992.
6. Gunter, E. J., O'Brien, J. T. and J. T. O'Brien, Jr. ***Experimental and Analytical Investigation of a Main Coolant Pump***, Sound and Vibration, May 1993, pp. 12 –24.
7. Kazoa, Y. and E. J. Gunter. ***Dynamics of Multi-Spool Gas Turbines Using the Transfer Matrix Method***, Proceedings of International Conference on Mechanical Dynamics, Press of Northeast University of Technology, Shenyang, Liaoning, China, August 1987.
8. ***MSC/pal2 Reference Manual*** (Ver. 4.0), The MacNeal Schwendler Corporation, Los Angeles, CA, 1990.
9. Nestorides, E. J. ***A Handbook on Torsional Vibration***, Cambridge Univ. Press, Cambridge, U.K., 1958.
10. Pestel, E. C. and F. H. Leckie. ***Matrix Methods in Elasto Mechanics***, McGraw Hill, New York, 1963.
11. Potts, J. F. and J. W. Oler. ***Finite Applications With Microcomputers***, Prentice Hall, Englewood Cliffs, NJ, 1989.
12. Potts, J. Editor, ***CDA/sprint Theory and Application Manual***, The CDA Group, Houston, TX, 1994.
13. Rao, S. S. ***Mechanical Vibrations***, Addison Wesley, Reading, MA, 1984.
14. Schwibinger, P., Feng, T., and R. Nordmann. ***Improvement of a Reduced Torsional Model by Means of Parameter Identification***, International Conference on Rotor Dynamics, Tokyo, Japan, Sept. 14–17, 1986, pp. 329–338.
15. Thompson, W. T. ***Theory of Vibrations With Applications***, Prentice Hall, Englewood Cliffs, NJ, 1988.
16. Timoshenko, S. and D. H. Young. ***Vibration Problems in Engineering***, D. Van Nostrand, Princeton, NJ, 1955.
17. Vance, J. M. ***Rotordynamics of Turbomachinery***, John Wiley, New York, 1988.
18. Wilson, W. Ken. ***Practical Solutions of Torsional Vibration Problems, Vol. 1–3***, Chapman & Hall Ltd., London U.K., 1963.